



# Effect of angulation on the 3D trueness of conventional and digital implant impressions for multi-unit restorations

Özay Önöral, Sevcan Kurtulmus-Yilmaz\*, Dilem Toksoy, Oguz Ozan

Department of Prosthodontics, Faculty of Dentistry, Near East University, Mersin10, Turkey

## ORCID

Özay Önöral

<https://orcid.org/0000-0002-5264-9376>

Sevcan Kurtulmus-Yilmaz

<https://orcid.org/0000-0001-8792-1977>

Dilem Toksoy

<https://orcid.org/0000-0002-2230-2822>

Oguz Ozan

<https://orcid.org/0000-0002-0119-1369>

**PURPOSE.** The study aimed to determine the influence of implant angulation on the trueness of multi-unit implant impressions taken through different techniques and strategies. **MATERIALS AND METHODS.** As reference models, three partially edentulous mandibular models (Model 1: No angulation; Model 2: No angulation for #33, 15-degree distal angulation for #35 and #37; Model 3: No angulation for #33, 25-degree distal angulation for #35 and #37) were created by modifying the angulations of implant analogues. Using a lab scanner, these reference models were scanned. The obtained data were preserved and utilized as virtual references. Three intraoral scanning (IOS) strategies: IOS-Omnicaam, ISO-Quadrant, and IOS-Consecutive, as well as two traditional techniques: splinted open tray (OT) and closed tray (CT), were used to create impressions from each reference model. The best-fit alignment approach was used to sequentially superimpose the reference and test scan data. Computations and statistical analysis of angular (AD), linear (LD), and 3D deviations (RMS) were performed. **RESULTS.** Model type, impression technique, as well as interaction factor, all demonstrated a significant influence on AD and LD values for all implant locations ( $P < .05$ ). The Model 1 and SOT techniques displayed the lowest mean AD and LD values across all implant locations. When considering interaction factors, CT-Model 3 and SOT-Model 1 exhibited the highest and lowest mean AD and LD values, respectively. Model type, impression technique, and interaction factor all revealed significant effects on RMS values ( $P \leq .001$ ). CT-Model 3 and SOT-Model 1 presented the highest and lowest mean RMS values, respectively. **CONCLUSION.** Splinted-OT and IOS-Omnicaam are recommended for multi-unit implant impressions to enhance trueness, potentially benefiting subsequent manufacturing stages. [J Adv Prosthodont 2023;15:290-301]

## KEYWORDS

Angulated implants; Closed tray; Splinted open tray; Intraoral scanners; Scan path

## Corresponding author

Sevcan Kurtulmus-Yilmaz  
Department of Prosthodontics,  
Faculty of Dentistry, Near East  
University, Nicosia, Cyprus, Mersin  
10, Turkey  
Tel +903926802030  
E-mail  
[sevcan.kurtulmus@neu.edu.tr](mailto:sevcan.kurtulmus@neu.edu.tr)

Received August 28, 2023 /

Last Revision November 27, 2023 /

Accepted December 15, 2023

© 2023 The Korean Academy of Prosthodontics

© This is an Open Access article distributed under the terms of the Creative Commons Attribution Non-Commercial License (<https://creativecommons.org/licenses/by-nc/4.0>) which permits unrestricted non-commercial use, distribution, and reproduction in any medium, provided the original work is properly cited.

## INTRODUCTION

Misfit of implant-supported restorations (ISRs) is defined as an instance of incongruent and disorderly contact at the juncture where the implant and the prosthetic superstructure meet. This culminates in static stress generation not only in the implant components but also in the surrounding bone and leads to a slew of mechanical and biological complications.<sup>1-3</sup> Therefore, achieving a misfit within the clinical acceptability range (passive fit) is for the long-term viability of ISRs.<sup>4</sup> This is especially critical for screw-retained ISRs as cement-retained counterparts necessitate a spacing of 25 to 50  $\mu\text{m}$  and this can lessen the strains brought on by less accurate restoration.<sup>3</sup> Several researchers have made attempts to quantify passive fit<sup>5,6</sup> Jemt<sup>7</sup> pointed out that a mismatch of 150  $\mu\text{m}$  was clinically tolerable. Because getting an absolute passive fit is almost unattainable, the best degree of fit is advised. Passive fit is only achievable with a precise prosthodontic process that begins with impression procedures.<sup>8,9</sup>

The misfit of an ISR is typically multifactorial.<sup>1</sup> When focused on the impression factor, the impression technique, impression material, number and alignment of implants, splinting or non-splinting impression copings, and subgingival depth of implants can all alter the accuracy of impression, thereby leading to increased discrepancy values at the interface due to the distortions occurred in the x-, y, and z-axes.<sup>1,4</sup> In ordinary circumstances, implant impressions are taken by employing the closed tray (CT) technique. However, in the clinical setting, proper implant positioning may not always be possible.<sup>10,11</sup> The lack of parallelism among implants might induce distortion of the elastomeric impression taken through the CT technique, resulting in an erroneous transfer.<sup>12</sup> Or, when an implant is positioned deeply subgingivally, the impression material might support a small portion of the impression coping, which can cause the coping to be displaced and compromise the accuracy of the impression.<sup>13,14</sup> In both cases, the splinted open tray (OT) (direct) technique is recommended as the most reliable and precise transfer method.<sup>15</sup>

In the past few decades, technological advances have been incorporated in dentistry, particularly for

the transfer of the spatial positions of the implants to a three-dimensional (3D) virtual model by utilizing computer-aided design and computer-aided manufacturing (CAD-CAM) technologies. As compared to traditional impression techniques, digital scanning performed using intraoral scanners (IOSs) has delivered clinically acceptable results in the fabrication of crowns and fixed restorations. This technique saves time, eliminates potential errors caused by the distortion of elastic impression materials and gypsum, exterminates the need for disinfection and transport to the dental laboratory, allows storage of scans, and promotes patient acceptance.<sup>16-18</sup>

Trueness and precision are the two components of accuracy. Trueness is the proximity of the test object to the reference object; on the other hand, precision is the fluctuation of the object's repetitive measurements.<sup>14,19-22</sup> An accurate scan is required for a successful prosthesis in a solely digital approach. In terms of accuracy, optical impressions for short-span restorations have been demonstrated to be similar to conventional impressions. Several investigations found that digital implant impressions are accurate to within 15.0 to 71.2  $\mu\text{m}$ , while clinical trials found errors that varied between 27.4 and 220  $\mu\text{m}$ .<sup>23</sup> A number of variables involving scanning length, scanning strategy, implant angulation, IOS types, operator experience, ambient light, IOS head size, scanner software program, and scan body types, have all been identified as potentially affecting the accuracy of digital data acquisition.<sup>16-18,24</sup>

Inaccuracies in digital implant impressions become more likely as the scanning length or interimplant distance gets longer, possibly due to accumulative faults in the IOS stitching process. The accuracy of digital scans across different edentulous span lengths has been scrutinized, and it has been highlighted that a longer edentulous span led to more mistakes.<sup>16,25-27</sup>

The so-called scanning strategy requires the clinician to maneuver the tip of the intraoral scanner along a predetermined path for proper scanning. Although Medina Sotomayor *et al.*<sup>28</sup> and Passos *et al.*<sup>29</sup> showed that the accuracy of IOS is affected by scan strategy, it is yet unclear how the scanning strategy might influence the accuracy of the impression. All scanning methods combine or stitch a number of con-

secutive images or videos obtained from various angles to form a 3D presentation.<sup>19,30</sup> The scan and the software used to stitch the images together are tightly interconnected; if the scanner moves too quickly or changes direction dramatically, the stitching process may be hampered.<sup>26,30</sup> Also, alternate scanning strategies other than those advised by the developer of the IOS might considerably reduce accuracy.<sup>30</sup> Anh *et al.*<sup>31</sup> proved that the beginning location of the scan affects how accurate the digital model is. The vertical rotation of the IOS should be avoided, according to Oh *et al.*<sup>32</sup>.

The conventional and digital impressions have been analyzed in terms of accuracy and conflicting results have been reported.<sup>14,33</sup> Some claimed that using traditional methods produced more accurate findings, however digital scans' accuracy was unaffected by angulation, and in nonparallel models, there were no appreciable differences between the two methods. Contrarily, Lin *et al.*<sup>34</sup> discovered that the OT technique had higher accuracy in the presence of only modest angular differences (0 - 15 degrees) between implants; however, when there was a significant degree of angular difference (30 - 45 degrees), digital scan groups provided superior results.

Clinicians face a decision making dilemma due to a lack of agreement on suggested impression techniques and scan strategies for angulated implants. To address this issue, in this study, it was aimed to compare the trueness of the intraoral scanning technique using three distinct scan strategies with those of conventional impression procedures for partially edentulous arches including angulated implants. The null hypotheses for this study were that the angulation of implants would not alter the trueness of impression techniques, that there would be no significant differences concerning the trueness of impression techniques, and that there would be no significant difference among scan strategies in terms of trueness.

## MATERIALS AND METHODS

The flowchart of this study is depicted in Figure 1. Before the commencement of the study, power analysis was used to establish the sample size. For the prior sample size calculation, software (G-Power, Version

3.1.9) was used and a medium effect size of 0.25 was estimated. At 85% power and a level of significance of 0.05, the total sample size for 15 groups matching this effect size was determined to be 277. A total sample size of 300 (20 for each group) was employed, yielding an overall power of 88.5%.

An autopolymerizing acrylic resin (Meliodent Rapid Repair Denture Acrylic, Kulzer GmbH, Hanau, Germany) was poured into the dentulous rubber mold (AG-3 Silicone Index; Frasco GmbH, Greenville, SC, USA) to obtain the definitive cast. The left posterior side starting from the right canine to the right 3rd molar was grinded to simulate partial edentulism with a healed ridge width of 8 mm. To fabricate 3 identical models, three impressions were made by using vinyl polysiloxane impression material (Elite HD+ Monophase; Zhermack, BadiaPosleine, Italy), and the same auto-polymerizing acrylic resin was poured into those impressions. Next, a rotary instrument was used to shape three implant sockets in the canine, 2nd premolar, and 2nd molar areas of all three casts. Multi-unit implant analogues (T0 32202, NucleOSS, İzmir, Turkey) were secured in their corresponding sockets with autopolymerizing acrylic resin. By varying implant angulations, three different models (Model 1: No angulation; Model 2: No angulation for #33, 15-degree distal angulation for #35 and #37; Model 3: No angulation for #33, 25-degree distal angulation for #35 and #37) were created and referred to as reference models. Polyetheretherketone (PEEK) scan bodies (T0 32033; NucleOSS, İzmir, Turkey) were screwed to the multi-unit implant analogues on each reference model. A laboratory scanner (inEOS X5, Dentsply Sirona, Charlotte, NC, USA) was used to scan the reference models, and the resulting data were saved in standard tessellation language (STL) format for use as virtual reference images.

For taking CT impressions, prefabricated metallic trays were utilized, and their internal surfaces were coated with tray adhesive (Universal Tray Adhesive; Zhermack, BadiaPosleine, Italy) and allowed to dry for two minutes. Subsequently, CT impression copings (T0 32607, NucleOSS, İzmir, Turkey) were manually screwed onto the multi-unit abutments on each reference model until resistance was felt, and then their corresponding caps (T0 32912, NucleOSS, İzmir,

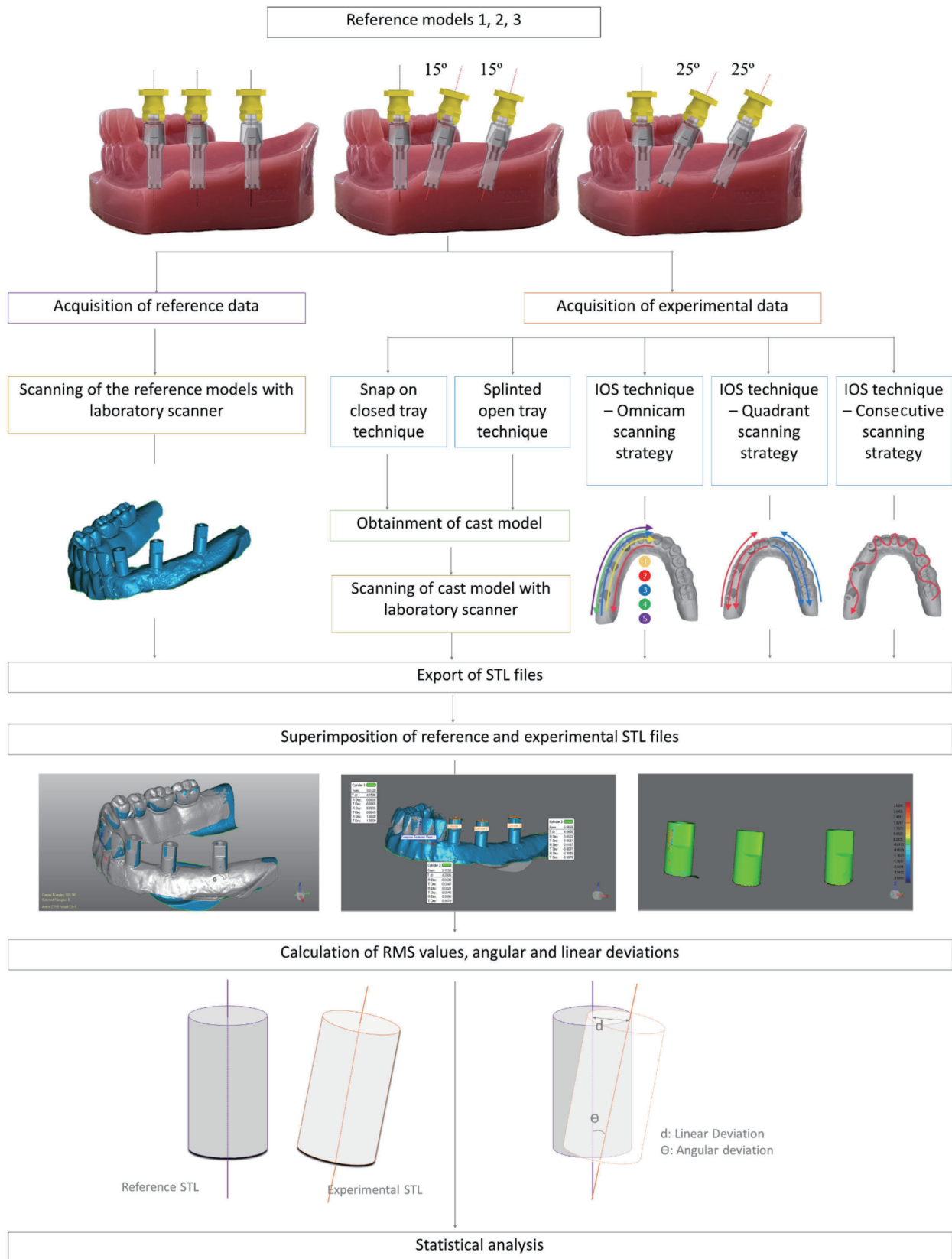


**Fig. 1.** Flowchart of this study. IOS technique, intraoral scanning technique; STL, standard tessellation language; RMS, root mean square.

Turkey) were affixed. A monophasic vinyl polysiloxane impression material (Elite HD+ Monophase) was then prepared and delivered through a syringe around the impression copings. The tray was loaded and positioned onto the reference model, where it was left for six minutes to be set. The CT impression copings were left in place on the reference model while the caps remained in the impression. Finally, the copings were unfastened, screwed to implant analogues, and placed into the caps that remained in the impression.

For taking OT impressions, non-hex OT impression copings (T0 32608, NucleOSS, İzmir, Turkey) were screwed onto the multi-unit implant analogues. Resin splints were created around the impression copings using dental floss and autopolymerizing acrylic resin (Pattern Resin LS, GC America Inc., Alsip, IL, USA). The splint was sectioned after 24 hours and rejoined with the same acrylic resin before the impression step. Customized impression trays were created by using light-cured base plates (Plaque Photo, W + P Dental, Hamburg, Germany) and polymerized (Tray Lux, Ampac Dental, Rockdale, Australia). These trays were drilled to access the coronal ends of the impression copings. Subsequently, tray adhesive was applied to their intaglio surfaces and allowed to cure for two minutes. Impression material was delivered through a syringe around the impression copings and the tray filled with impression material was placed onto the reference models. The impression material had been left to polymerize for six minutes. While the impression was still on the reference model, the OT impression copings were unfastened by accessing the connecting screw through the drilled holes on the trays. The tray, along with the copings, was taken off the model and copings were secured to the implant analogues before pouring.

All of these steps were done by a single calibrated clinician and in total, 120 conventional impressions ( $n = 20$  for each model) were made. To create the test casts, a type IV dental stone (GC Fujirock EP, GC Corp., Tokyo, Japan) was used to pour up all conventional impressions. The castings and impressions were separated after 24 hours. On the test casts, PEEK scan bodies were fastened to the analogs. The same lab scanner was utilized for all scans, and the data was exported into the STL format for use as virtual test im-

ages.

A calibrated clinician conducted the digital impression procedures by using an intraoral scanner (CEREC Omnicam, Dentsply Sirona, software version: CEREC SW) in this study. For each reference model, ten digital impressions were acquired by using PEEK scan bodies compatible with the multi-unit abutments. The scans were performed in 3 different strategies, as specified below, and the STL-formatted scans were all preserved and utilized as virtual test imagery.

- **IOS-Omnicam:** This is in accordance with the scanning strategy recommended by the Omnicam manufacturer. It was started by scanning the occlusal surface of the scan-bodies on the implantation site. The scanner tip was guided from the distal to the mesial by palatally tilting it by 45 degrees. The header was moved in a distal direction while tilting it an additional 45 degrees in the palatal direction. Then, it was moved in a mesial way while tilting it 90 degrees toward the occlusal surface. It was turned 45 degrees buccal and advanced backward toward the distal. Next, it was tilted a further 45 degrees in the buccal direction to a total of 90 degrees and moved in the mesial direction.
- **IOS-Quadrant:** Two quadrants of the model were separately scanned. Starting from the midline and moving posteriorly, the model was occlusally scanned. The header was turned over to the buccal side, and the midline was reached by scanning from the back to the front. The header was then flipped over to the lingual side and scanned from the midline to the posterior area. The opposite quadrant underwent the same procedure. Scanning was started from the implantation site.
- **IOS-Consecutive:** Scanning was started from the dentulous site and continued by making a zigzag motion on the occlusal-buccal-occlusal-lingual path.

Geomagic Control (3D Systems, Rock Hill, SC, USA), a 3D metrology program, was utilized by a single operator for performing 3D analysis on all STL data. A best-fit alignment technique was used to align the reference and test scan data, and the resulting 3D deviation was investigated. The algorithm was instructed to use the best-fit alignment from the dentulous

side of the model to minimize the amount of deviation during superimposition. Root mean square (RMS) error was evaluated to ascertain how well these datasets matched. A more accurate alignment is indicated by lower RMS error levels.

To evaluate 3D discrepancies between the test data and the reference data, color maps were generated using the software's 3D comparison algorithm. The maximum/minimum deviation values were set at +100/-100  $\mu\text{m}$ , and a tolerance interval of +50/-50  $\mu\text{m}$  was utilized to quantify the data as the mean and standard deviation (SD). The software automatically provided the RMS values from the maps without the requirement for further calculation. This study aimed to find 3D deviation on scan bodies; hence RMS values were only computed for the scan bodies and not for the complete models.

Virtual scan bodies on the reference scan data were converted into virtual hollow cylinders using the feature creation tab. The autocreate tab was then utilized to create identical cylinders on the test scan data for uniformity. The center lines running through these cylinders were measured by using their directional cartesian coordinates ( $x$ ,  $y$ , and  $z$ ). According to the following formulae, the linear (LD) and angular deviations (AD) between the test and reference cylinders' center lines were calculated:

$$LD = \sqrt{((X^1 - X^2)^2 + (Y^1 - Y^2)^2 + (Z^1 - Z^2)^2)}$$

$$AD = (\arccos[(X_1 \times X_2) + (Y_1 \times Y_2) + (Z_1 \times Z_2)] / ((\sqrt{(X_1^2 + Y_1^2 + Z_1^2)} \times \sqrt{(X_2^2 + Y_2^2 + Z_2^2)})))$$

where the coordinates of the line on the reference data are  $X_1$ ,  $Y_1$ , and  $Z_1$ ; while the coordinates of the line on the test data are  $X_2$ ,  $Y_2$ , and  $Z_2$ .

Software for statistical analysis (SPSS Statistics 25.0, SPSS Inc., Chicago, IL, USA) was used to process the data. Before analysis, the Shapiro-Wilk test was used to verify that the data collected for linear deviation, angular deviation, and RMS estimate had a normal distribution. The data was then analyzed using a two-way analysis of variance (ANOVA) with a significance level of 0.05, followed by one-way ANOVA and Tukey Post Hoc comparison tests.

## RESULTS

According to the findings of the two-way ANOVA, the model type, impression technique, and interaction term had a significant influence on AD and LD values for all implant locations ( $P < .05$  for AD and LD) (Table 1 and Table 2). The Model 1 and splinted-OT techniques had the lowest mean AD and LD values for all implant locations. Regarding the model type, Model 3 and Model 1 had the highest and lowest mean values, respectively. There were statistically significant differences in all models ( $P < .05$ ). IOS-Quadrant had the largest deviation values for the impression technique, with the exception of AD of #37, AD of #35, and LD of #35. CT demonstrated the largest deviation values for these measurements. Splinted-OT showed statistically lower AD and LD values than all other groups ( $P < .05$ ). The CT-Model 3 and SOT-Model 1 had the highest and the lowest mean AD and LD values, respectively, when interaction was taken into account.

The results of 2-way ANOVA showed that model type ( $P \leq .001$ ), impression technique ( $P \leq .001$ ), and their interaction terms ( $P \leq .001$ ) significantly influenced RMS estimate values. Table 3 displays the mean RMS estimate values and standard deviations with Tukey post hoc comparisons. In terms of model type, Model 3 and Model 1 had the highest and the lowest mean RMS values, respectively. There were statistically significant differences among models. In terms of impression technique, IOS-Quadrant had the greatest RMS value, followed by CT, IOS-Consecutive, IOS-Omniscam, and splinted-OT. Furthermore, the RMS value for splinted-OT was determined to be much lower than others. The CT-Model 3 and splinted OT-Model 1 had the highest and lowest mean RMS values, respectively, once the interaction term was considered.

## DISCUSSION

The adoption of intraoral scanners is growing, but there isn't enough evidence to conclude if digital impressions are more accurate than traditional ones, especially when implants aren't ideally positioned. Therefore, in this study, the angular, linear, and 3D deviations of the scan bodies on the computerized models generated through digital and conventional

**Table 1.** Angular deviation (degrees) values and standard deviations with Tukey Post Hoc comparisons

Impression Techniques	Models			
	Model 1	Model 2	Model 3	Total
<b>Implant #33</b>				
Splinted open tray	0.00 ± 0.00 <sup>a,A</sup>	0.00 ± 0.00 <sup>a,A</sup>	0.01 ± 0.02 <sup>a,A</sup>	0.00 ± 0.01 <sup>a</sup>
Closed tray	0.00 ± 0.00 <sup>a,A</sup>	0.06 ± 0.09 <sup>ab,A</sup>	0.58 ± 0.08 <sup>c,B</sup>	0.21 ± 0.28 <sup>b</sup>
IOS-Omnacam	0.24 ± 0.11 <sup>ab,A</sup>	0.29 ± 0.09 <sup>b,A</sup>	0.31 ± 0.27 <sup>b,A</sup>	0.28 ± 0.17 <sup>b</sup>
IOS-Quadrant	0.29 ± 0.08 <sup>b,A</sup>	0.53 ± 0.21 <sup>c,B</sup>	0.69 ± 0.19 <sup>c,B</sup>	0.50 ± 0.23 <sup>c</sup>
IOS-Consecutive	0.27 ± 0.14 <sup>b,A</sup>	0.52 ± 0.26 <sup>c,B</sup>	0.61 ± 0.19 <sup>c,B</sup>	0.47 ± 0.24 <sup>c</sup>
Total	0.16 ± 0.16 <sup>A</sup>	0.28 ± 0.27 <sup>B</sup>	0.44 ± 0.30 <sup>C</sup>	0.29 ± 0.27
<b>Implant #35</b>				
Splinted open tray	0.18 ± 0.06 <sup>a,A</sup>	0.24 ± 0.07 <sup>a,A</sup>	0.41 ± 0.10 <sup>a,A</sup>	0.28 ± 0.12 <sup>a</sup>
Closed tray	0.24 ± 0.08 <sup>a,A</sup>	0.70 ± 0.14 <sup>b,B</sup>	1.14 ± 0.20 <sup>c,C</sup>	0.69 ± 0.40 <sup>c</sup>
IOS-Omnacam	0.29 ± 0.17 <sup>a,A</sup>	0.50 ± 0.27 <sup>ab,AB</sup>	0.71 ± 0.16 <sup>ab,B</sup>	0.50 ± 0.26 <sup>b</sup>
IOS-Quadrant	0.39 ± 0.15 <sup>a,A</sup>	0.80 ± 0.20 <sup>b,B</sup>	0.94 ± 0.27 <sup>bc,B</sup>	0.71 ± 0.31 <sup>c</sup>
IOS-Consecutive	0.29 ± 0.12 <sup>a,A</sup>	0.41 ± 0.25 <sup>a,A</sup>	0.55 ± 0.18 <sup>a,A</sup>	0.42 ± 0.21 <sup>ab</sup>
Total	0.28 ± 0.13 <sup>A</sup>	0.53 ± 0.28 <sup>B</sup>	0.75 ± 0.32 <sup>C</sup>	0.52 ± 0.32
<b>Implant #37</b>				
Splinted open tray	0.22 ± 0.05 <sup>a,A</sup>	0.28 ± 0.13 <sup>a,A</sup>	0.43 ± 0.10 <sup>a,A</sup>	0.31 ± 0.13 <sup>a</sup>
Closed tray	0.31 ± 0.13 <sup>a,A</sup>	0.78 ± 0.09 <sup>b,B</sup>	1.24 ± 0.26 <sup>c,C</sup>	0.78 ± 0.43 <sup>b</sup>
IOS-Omnacam	0.33 ± 0.21 <sup>a,A</sup>	0.41 ± 0.12 <sup>a,AB</sup>	0.60 ± 0.17 <sup>a,B</sup>	0.45 ± 0.19 <sup>a</sup>
IOS-Quadrant	0.43 ± 0.19 <sup>a,A</sup>	0.71 ± 0.22 <sup>b,B</sup>	0.81 ± 0.15 <sup>b,B</sup>	0.65 ± 0.24 <sup>b</sup>
IOS-Consecutive	0.37 ± 0.09 <sup>a,A</sup>	0.41 ± 0.21 <sup>a,A</sup>	0.47 ± 0.10 <sup>a,A</sup>	0.41 ± 0.14 <sup>a</sup>
Total	0.33 ± 0.15 <sup>A</sup>	0.52 ± 0.25 <sup>B</sup>	0.71 ± 0.34 <sup>C</sup>	0.52 ± 0.30

Different superscript lowercase letters indicate significant differences in the same column; Different superscript uppercase letters indicate significant differences in the same row. Only the significant differences among experimental groups were given as superscript letters.

impression techniques were tracked. Statistical analyses utilized in this study revealed that impression technique, scanning strategy, and implant angulation had a significant effect on the trueness of the impressions; therefore, all null hypotheses were rejected.

The transfer of implant locations should be accurate in order for the disparity to be compensated by the resilience of the bone, the residual mobility of the implants, and the machining tolerances of the abutments.<sup>35</sup> In terms of passive fit, ISRs with discrepancies as small as 10 µm service better;<sup>6</sup> nevertheless, a misfit classification created by using current fabrication procedures deemed interface discrepancies up to 100 µm to be clinically acceptable.<sup>3</sup> Discrepancy assessment has not been done in this study. As a result, the current study's findings could not be evaluated using the specified thresholds. Assuncao *et al.*<sup>12</sup> reported that a discrepancy of 50 µm along any axis

is tolerable in a good impression and can be utilized to digitize the trueness. The clinical tolerance criterion for angular deviations is also missing. However, it has been argued that up to 0.4° angular deviation might be acceptable by considering basic trigonometric functions and assuming that the maximum lateral apex movement of 50 µm is acceptable.<sup>17,36</sup> When the RMS estimate values were investigated, it was understood that the values for all impression techniques in Model 1 were well-below 50 µm. The RMS estimate values of the splinted-OT, IOS-Omnacam, and IOS-Consecutive for Model 2 and the splinted-OT for Model 3 were below that threshold. When the angular deviation values were examined, it was observed that the values for all impression techniques in Model 1 were 0.4 degree and below. As the implant angles increased in other models, many values exceeded the above-mentioned threshold value. Splinted-OT tech-

**Table 2.** Linear deviation ( $\mu\text{m}$ ) values and standard deviations with Tukey Post Hoc comparisons

Impression Techniques	Models			
	Model 1	Model 2	Model 3	Total
<b>Implant #33</b>				
Splinted open tray	0.0000 $\pm$ 0.0000 <sup>a,A</sup>	0.0000 $\pm$ 0.0000 <sup>a,A</sup>	0.0002 $\pm$ 0.0003 <sup>a,A</sup>	0.0001 $\pm$ 0.0002 <sup>a</sup>
Closed tray	0.0000 $\pm$ 0.0000 <sup>a,A</sup>	0.0012 $\pm$ 0.0000 <sup>a,A</sup>	0.0104 $\pm$ 0.0014 <sup>c,B</sup>	0.0039 $\pm$ 0.0049 <sup>b</sup>
IOS-Omnica	0.0043 $\pm$ 0.0020 <sup>ab,A</sup>	0.0051 $\pm$ 0.0017 <sup>b,A</sup>	0.0054 $\pm$ 0.0048 <sup>b,A</sup>	0.0049 $\pm$ 0.0030 <sup>b</sup>
IOS-Quadrant	0.0051 $\pm$ 0.0015 <sup>b,A</sup>	0.0093 $\pm$ 0.0036 <sup>bc,B</sup>	0.0120 $\pm$ 0.0034 <sup>c,B</sup>	0.0088 $\pm$ 0.0040 <sup>c</sup>
IOS-Consecutive	0.0047 $\pm$ 0.0026 <sup>b,A</sup>	0.0092 $\pm$ 0.0045 <sup>bc,B</sup>	0.0107 $\pm$ 0.0033 <sup>c,B</sup>	0.0082 $\pm$ 0.0042 <sup>c</sup>
Total	0.0028 $\pm$ 0.0028 <sup>A</sup>	0.0050 $\pm$ 0.0047 <sup>B</sup>	0.0077 $\pm$ 0.0053 <sup>C</sup>	0.0052 $\pm$ 0.0048
<b>Implant #35</b>				
Splinted open tray	0.0040 $\pm$ 0.0020 <sup>a,A</sup>	0.0051 $\pm$ 0.0012 <sup>a,A</sup>	0.0085 $\pm$ 0.0026 <sup>a,A</sup>	0.0059 $\pm$ 0.0027 <sup>a</sup>
Closed tray	0.0043 $\pm$ 0.0013 <sup>a,A</sup>	0.0124 $\pm$ 0.0024 <sup>bc,B</sup>	0.0224 $\pm$ 0.0074 <sup>c,C</sup>	0.0131 $\pm$ 0.0087 <sup>c</sup>
IOS-Omnica	0.0051 $\pm$ 0.0030 <sup>a,A</sup>	0.0115 $\pm$ 0.0048 <sup>bc,B</sup>	0.0124 $\pm$ 0.0028 <sup>bc,B</sup>	0.0097 $\pm$ 0.0048 <sup>bc</sup>
IOS-Quadrant	0.0069 $\pm$ 0.0026 <sup>a,A</sup>	0.0144 $\pm$ 0.0032 <sup>c,B</sup>	0.0166 $\pm$ 0.0047 <sup>c,B</sup>	0.0126 $\pm$ 0.0055 <sup>c</sup>
IOS-Consecutive	0.0051 $\pm$ 0.0022 <sup>a,A</sup>	0.0079 $\pm$ 0.0038 <sup>ab,AB</sup>	0.0111 $\pm$ 0.0030 <sup>ab,BC</sup>	0.0080 $\pm$ 0.0038 <sup>ab</sup>
Total	0.0051 $\pm$ 0.0023 <sup>A</sup>	0.0102 $\pm$ 0.0046 <sup>B</sup>	0.0142 $\pm$ 0.0065 <sup>C</sup>	0.0098 $\pm$ 0.0060
<b>Implant #37</b>				
Splinted open tray	0.0042 $\pm$ 0.0007 <sup>a,A</sup>	0.0054 $\pm$ 0.0019 <sup>a,AB</sup>	0.0086 $\pm$ 0.0020 <sup>a,B</sup>	0.0061 $\pm$ 0.0025 <sup>a</sup>
Closed tray	0.0057 $\pm$ 0.0022 <sup>a,A</sup>	0.0140 $\pm$ 0.0017 <sup>b,B</sup>	0.0243 $\pm$ 0.0050 <sup>c,C</sup>	0.0147 $\pm$ 0.0084 <sup>b</sup>
IOS-Omnica	0.0059 $\pm$ 0.0037 <sup>a,A</sup>	0.0078 $\pm$ 0.0025 <sup>a,AB</sup>	0.0105 $\pm$ 0.0030 <sup>ab,B</sup>	0.0080 $\pm$ 0.0035 <sup>a</sup>
IOS-Quadrant	0.0079 $\pm$ 0.0036 <sup>a,A</sup>	0.0135 $\pm$ 0.0030 <sup>b,B</sup>	0.0147 $\pm$ 0.0029 <sup>b,B</sup>	0.0120 $\pm$ 0.0042 <sup>b</sup>
IOS-Consecutive	0.0065 $\pm$ 0.0013 <sup>a,A</sup>	0.0072 $\pm$ 0.0036 <sup>a,A</sup>	0.0085 $\pm$ 0.0019 <sup>a,A</sup>	0.0074 $\pm$ 0.0024 <sup>a</sup>
Total	0.0060 $\pm$ 0.0027 <sup>A</sup>	0.0096 $\pm$ 0.0043 <sup>B</sup>	0.0133 $\pm$ 0.0067 <sup>C</sup>	0.0096 $\pm$ 0.0056

Different superscript lowercase letters indicate significant differences in the same column; Different superscript uppercase letters indicate significant differences in the same row. Only the significant differences among experimental groups were given as superscript letters.

**Table 3.** RMS estimate values and standard deviations with Tukey Post Hoc comparisons

Impression Techniques	Models			
	Model 1	Model 2	Model 3	Total
Splinted open tray	18.08 $\pm$ 3.96 <sup>a,A</sup>	21.82 $\pm$ 4.98 <sup>a,AB</sup>	34.05 $\pm$ 3.48 <sup>a,B</sup>	24.65 $\pm$ 8.05 <sup>a</sup>
Closed tray	24.26 $\pm$ 4.11 <sup>ab,A</sup>	57.38 $\pm$ 6.33 <sup>b,B</sup>	104.50 $\pm$ 12.19 <sup>d,C</sup>	62.04 $\pm$ 34.93 <sup>c</sup>
IOS-Omnica	34.22 $\pm$ 11.63 <sup>abc,A</sup>	46.02 $\pm$ 11.63 <sup>b,AB</sup>	59.55 $\pm$ 11.93 <sup>b,B</sup>	46.60 $\pm$ 15.25 <sup>b</sup>
IOS-Quadrant	42.94 $\pm$ 7.31 <sup>c,A</sup>	74.04 $\pm$ 15.85 <sup>c,B</sup>	87.84 $\pm$ 7.30 <sup>c,B</sup>	68.27 $\pm$ 21.91 <sup>c</sup>
IOS-Consecutive	36.68 $\pm$ 7.99 <sup>bc,A</sup>	50.04 $\pm$ 5.78 <sup>b,AB</sup>	60.38 $\pm$ 10.44 <sup>b,B</sup>	49.03 $\pm$ 12.64 <sup>b</sup>
Total	31.24 $\pm$ 11.42 <sup>A</sup>	49.86 $\pm$ 19.53 <sup>B</sup>	69.26 $\pm$ 26.51 <sup>C</sup>	50.12 $\pm$ 25.26 <sup>a</sup>

Different superscript lowercase letters indicate significant differences in the same column; Different superscript uppercase letters indicate significant differences in the same row. Only the significant differences among experimental groups were given as superscript letters.

nique has proven to be the most reliable impression technique by not exceeding the threshold value in all 3 models.

CT and splinted-OT were two conventional procedures used in the current study. Several implant companies have come up with the snap-fit (press-fit) in-

direct impression technique for transferring implant orientation to the cast model. The press-fit technique design enables the removal of copings within the impression and benefits from both CT and OT impression procedures.<sup>37</sup> According to a review,<sup>13</sup> clinically acceptable impressions may be made in the presence



of two or three implants by using both OT and CT procedures, and a prior study<sup>9</sup> indicated that both techniques yield accurate impressions for three implants angulated up to 15 degrees. Of conventional techniques, the splinted-OT technique showed superior accuracy than the CT technique in the presence of both parallel and tilted implants. This provides consistency with other studies.<sup>38-40</sup> The deformation of impression material during tray removal may explain the CT technique's inaccuracy in angulated models. Furthermore, various challenges, such as connecting the implant analog to the impression coping, or faults, such as plastic cap deformation, may have an impact on the accuracy of this approach. The splinted-OT impression was shown to have higher trueness than IOS groups as well and this finding is in line with those of Alsharbaty *et al.*<sup>41</sup> and Kim *et al.*<sup>42</sup> However, Abduo and Palamara<sup>43</sup> reported that digital technique typically yields more precise results than traditional techniques. This proves that there is still no agreement among researchers comparing the accuracy of traditional and digital impression techniques as to which method is better.

As the risks such as distortion of impression material and displacement of the impression coping are eradicated in digital scans, the accuracy of digital impressions is assumed not to be influenced by angular alterations among implants.<sup>14,44</sup> Previous studies have argued that tilting the implant may be advantageous as tilting the posterior implant mesially shortens the distance of the edentulous region between scan bodies, leading to better data acquisition.<sup>45</sup> However, digital impressions in angulated models had much greater deviation values in the current study in comparison to the splinted-OT technique. This finding may be attributed to the increase in the distance between scan bodies due to the distal angulation of the implants. Additional inquiry is required to reflect the effectiveness of digital impressions in the case of angulated implants.

For each intraoral impression device, companies have come up with distinctive scan strategies based on the software capabilities and capture technology. Numerous scientific studies have examined how crucial it is to adhere to a scanning strategy in order to get reliable scans.<sup>19</sup> The current study demonstrat-

ed that various scanning strategies had an impact on the impression trueness. Although this provides consistency with several studies;<sup>29-31</sup> Medina-Sotomayor *et al.*<sup>28</sup> expressed a dissenting outcome. When scanning strategies were compared, it was concluded that the STOmnicam exhibited higher trueness than the IOS-Quadrant and IOS-Consecutive. It has been highlighted that scanning strategies other than those recommended by the IOS's developer may significantly lessen accuracy. This reinforces the superiority of the strategy proposed by Omnicam. In the IOS-Consecutive and IOS-Quadrant strategies, higher deviation values have been found. In the IOS-Consecutive, scanning was not started from the implant site. This may lead to the reflection of accumulative faults in the IOS stitching process, similar to the previous study.<sup>10</sup> In the IOS-Quadrant, there may be an error in merging the images acquired from two separate quadrants in the anterior region.

Substantial innovations in computer-aided dentistry have led to the launch of various 3D superimposition services. The recently released best-fit-alignment algorithm has enabled the superimposition of computer-generated datasets to analyze accuracy through the RMS estimate value, which is calculated from the average distances of all point clouds in the superimposed reference and test models.<sup>14,16</sup> The best-fit-alignment method, on the other hand, operates by matching a set of measured points, as nearly as feasible, to that of their counterpart. As a result, the real positional interplay between the reference and test datasets may diverge far more, and the deviation between the virtual visualizations may be misinterpreted. To avoid this consequence, superimposition software was compelled to perform the function of best-fit-alignment in this study by picking the dentulous area and therefore eliminating the partially edentulous span at which implantation was performed. To provide more accurate and exact findings, 3D superimposition software was instructed to compute the RMS estimate value solely from the scan bodies rather than the entire model.

When referring to implant impression materials, polyether and vinyl polysiloxane are highly recommended.<sup>13</sup> Polyether provides good service in totally edentulous and multi-implant instances because of

its dimensional stability and rigidity.<sup>46</sup> However, owing to its rigid nature, antagonistic factors interact. On the one hand, its rigidity aids in holding the impression coping in place and preventing any displacement.<sup>15</sup> Tray removal, on the other hand, becomes tough.<sup>46</sup> With this intention, it would be more rational to utilize a material with better elastic recovery, such as vinyl polysiloxane, specifically when faced with nonparallel and internal connection implants. As a result, permanent deformation can be diminished since less tension accumulates between the impression copings and the material.<sup>46</sup> Accordingly, vinyl polysiloxane was chosen in this study.

This study has several limitations. The intraoral scanning was not carried out in a dimly lit setting, such as the inside of the mouth. The illumination was assumed to have an impact on the outcomes. PEEK scan bodies were utilized. Different results may be obtained when using titanium scan bodies. In angled models, the implants are tilted distally. The results could have changed if the implants were angled mesially. Only a single type of impression material and intraoral scanner were utilized, and the results may change depending on the materials and technologies employed. Three common scanning strategies were included, but different strategies may offer different trueness values. Prosthetic frameworks should be fabricated to provide more clinically meaningful outcomes while comparing different impression procedures. This attempt can analyze not only the fit of the frameworks but also the association between discrepancies and deviations. As a result, further inquiry is required.

## CONCLUSION

Within the limitations of this study, it can be concluded that angulation differences among implants have a significant impact on the trueness of implant impressions. All impression techniques were found reliable when implants were placed parallel to each other. However, when dealing with non-parallel implants, the study suggests that the open-tray impression technique, in combination with the splinting non-hex impression copings, can improve the trueness of the impression. Additionally, the study found that the

chosen scan strategy has a significant influence on the trueness of intraoral scans. It may be suggested that following the scanning strategy recommended by the manufacturer results in higher levels of trueness.

## REFERENCES

1. Kan JY, Rungcharassaeng K, Bohsali K, Goodacre CJ, Lang BR. Clinical methods for evaluating implant framework fit. *J Prosthet Dent* 1999;81:7-13.
2. Sahin S, Cehreli MC. The significance of passive framework fit in implant prosthodontics: current status. *Implant Dent* 2001;10:85-92.
3. Katsoulis J, Takeichi T, Sol Gaviria A, Peter L, Katsoulis K. Misfit of implant prostheses and its impact on clinical outcomes. Definition, assessment and a systematic review of the literature. *Eur J Oral Implantol* 2017;10:121-38.
4. Richi MW, Kurtulmus-Yilmaz S, Ozan O. Comparison of the accuracy of different impression procedures in case of multiple and angulated implants. *Head Face Med* 2020;16:1-12.
5. Klineberg IJ, Murray GM. Design of superstructures for osseointegrated fixtures. *Swed Dent J Suppl* 1985;28:63-9.
6. Brånemark PI. Osseointegration and its experimental background. *J Prosthet Dent* 1983;50:399-410.
7. Jemt T. Failures and complications in 391 consecutively inserted fixed prostheses supported by Brånemark implants in edentulous jaws: a study of treatment from the time of prosthesis placement to the first annual checkup. *Int J Oral Maxillofac Implants* 1991;6:270-6.
8. Abduo J, Bennani V, Waddell N, Lyons K, Swain M. Assessing the fit of implant fixed prostheses: a critical review. *Int J Oral Maxillofac Implants* 2010;25:506-15.
9. Conrad HJ, Pesun IJ, DeLong R, Hodges JS. Accuracy of two impression techniques with angulated implants. *J Prosthet Dent* 2007;97:349-56.
10. Lee H, Ercoli C, Funkenbusch PD, Feng C. Effect of subgingival depth of implant placement on the dimensional accuracy of the implant impression: an in vitro study. *J Prosthet Dent* 2008;99:107-13.
11. Laohverapanich K, Luangchana P, Anunmana C, Pornprasertsuk-Damrongsri S. Different implant subgingi-

- val depth affects the trueness and precision of the 3d dental implant position: a comparative in vitro study among five digital scanners and a conventional technique. *Int J Oral Maxillofac Implants* 2021;36:1111-20.
12. Assuncao WG, Filho HG, Zaniquelli O. Evaluation of transfer impressions for osseointegrated implants at various angulations. *Implant Dent* 2004;13:358-66.
  13. Lee H, So JS, Hochstedler JL, Ercoli C. The accuracy of implant impressions: a systematic review. *J Prosthet Dent* 2008;100:285-91.
  14. Chia VA, Esguerra RJ, Teoh KH, Teo JW, Wong KM, Tan KB. In vitro three-dimensional accuracy of digital implant impressions: the effect of implant angulation. *Int J Oral Maxillofac Implants* 2017;32:313-21.
  15. Moreira AH, Rodrigues NF, Pinho AC, Fonseca JC, Vilaça JL. Accuracy comparison of implant impression techniques: a systematic review. *Clin Implant Dent Relat Res* 2015;17 Suppl 2:e751-64.
  16. Sanda M, Miyoshi K, Baba K. Trueness and precision of digital implant impressions by intraoral scanners: a literature review. *Int J Implant Dent* 2021;7:1-25.
  17. Spitznagel F, Horvath S, Gierthmuehlen P. Prosthetic protocols in implant-based oral rehabilitations: A systematic review on the clinical outcome of monolithic all-ceramic single- and multi-unit prostheses. *Eur J Oral Implant* 2017;10:89-99.
  18. Papaspyridakos P, Vazouras K, Chen YW, Kotina E, Natto Z, Kang K, Chochlidakis K. Digital vs conventional implant impressions: a systematic review and meta-analysis. *J Prosthodont* 2020;29:660-78.
  19. Robles-Medina M, Romeo-Rubio M, Salido MP, Pradíes G. Digital intraoral impression methods: an update on accuracy. *Curr Oral Heal Rep* 2020;7:361-75.
  20. Gómez-Polo M, Álvarez F, Ortega R, Gómez-Polo C, Barmak AB, Kois JC, Revilla-León M. Influence of the implant scan body bevel location, implant angulation and position on intraoral scanning accuracy: An in vitro study. *J Dent* 2022;121:104122.
  21. Revilla-León M, Att W, Özcan M, Rubenstein J. Comparison of conventional, photogrammetry, and intraoral scanning accuracy of complete-arch implant impression procedures evaluated with a coordinate measuring machine. *J Prosthet Dent* 2021;125:470-8.
  22. Rotar RN, Faur AB, Pop D, Jivanescu A. Scanning distance influence on the intraoral scanning accuracy-an in vitro study. *Materials (Basel)* 2022;15:3061.
  23. Zhang YJ, Qiao SC, Qian SJ, Zhang CN, Shi JY, Lai HC. Influence of different factors on the accuracy of digital impressions of multiple implants: an in vitro study. *Int J Oral Maxillofac Implants* 2021;36:442-9.
  24. Alikhasi M, Alsharbaty MHM, Moharrami M. Digital Implant impression technique accuracy: a systematic review. *Implant Dent* 2017;26:929-35.
  25. Marques S, Ribeiro P, Falcão C, Lemos BF, Ríos-Carrasco B, Ríos-Santos JV, Herrero-Climent M. Digital impressions in implant dentistry: a literature review. *Int J Environ Res Public Health* 2021;18:1020.
  26. An H, Langas EE, Gill AS. Effect of scanning speed, scanning pattern, and tip size on the accuracy of intraoral digital scans. *J Prosthet Dent* 2022:S0022-3913(22)00326-2.
  27. Cortes ARG, Agius A-M, No-Cortes J. Factors affecting trueness of intraoral scans: an update. *Appl Sci* 2022;12:6675.
  28. Medina-Sotomayor P, Pascual-Moscardó A, Camps I. Accuracy of four digital scanners according to scanning strategy in complete-arch impressions. *PLoS One* 2018;13:e0202916.
  29. Passos L, Meiga S, Brigagão V, Street A. Impact of different scanning strategies on the accuracy of two current intraoral scanning systems in complete-arch impressions: an in vitro study. *Int J Comput Dent* 2019;22:307-19.
  30. Gavounelis NA, Gogola CC, Halazonetis DJ. The effect of scanning strategy on intraoral scanner's accuracy. *Dent J (Basel)* 2022;10:123.
  31. Anh JW, Park JM, Chun YS, Kim M, Kim M. A comparison of the precision of three-dimensional images acquired by 2 digital intraoral scanners: effects of tooth irregularity and scanning direction. *Korean J Orthod* 2016;46:3-12.
  32. Oh KC, Park JM, Moon HS. Effects of scanning strategy and scanner type on the accuracy of intraoral scans: a new approach for assessing the accuracy of scanned data. *J Prosthodont* 2020;29:518-23.
  33. Basaki K, Alkumru H, De Souza G, Finer Y. Accuracy of digital vs conventional implant impression approach: a three-dimensional comparative in vitro analysis. *Int J Oral Maxillofac Implants* 2017;32:792-9.
  34. Lin WS, Harris BT, Elathamna EN, Abdel-Azim T, Morton D. Effect of implant divergence on the accuracy of definitive casts created from traditional and digi-

- tal implant-level impressions: an in vitro comparative study. *Int J Oral Maxillofac Implants* 2015;30:102-9.
35. Schmidt A, Rein PE, Wöstmann B, Schlenz MA. A comparative clinical study on the transfer accuracy of conventional and digital implant impressions using a new reference key-based method. *Clin Oral Implants Res* 2021;32:460-9.
  36. Andriessen FS, Rijkens DR, van der Meer WJ, Wismeijer DW. Applicability and accuracy of an intraoral scanner for scanning multiple implants in edentulous mandibles: a pilot study. *J Prosthet Dent* 2014;111:186-94.
  37. Tsagkalidis G, Tortopidis D, Mpikos P, Kaisarlis G, Koidis P. Accuracy of 3 different impression techniques for internal connection angulated implants. *J Prosthet Dent* 2015;114:517-23.
  38. Stimmelmayer M, Erdelt K, Güth JF, Happe A, Beuer F. Evaluation of impression accuracy for a four-implant mandibular model--a digital approach. *Clin Oral Investig* 2012;16:1137-42.
  39. Kurtulmus-Yilmaz S, Ozan O, Ozelik TB, Yagiz A. Digital evaluation of the accuracy of impression techniques and materials in angulated implants. *J Dent* 2014;42:1551-9.
  40. Elshenawy EA, Alam-Eldein AM, Abd Elfatah FA. Cast accuracy obtained from different impression techniques at different implant angulations (in vitro study). *Int J Implant Dent* 2018;4:9.
  41. Alsharbaty MHM, Alikhasi M, Zarrati S, Shamshiri AR. A clinical comparative study of 3-dimensional accuracy between digital and conventional implant impression techniques. *J Prosthodont* 2019;28:e902-8.
  42. Kim KR, Seo KY, Kim S. Conventional open-tray impression versus intraoral digital scan for implant-level complete-arch impression. *J Prosthet Dent* 2019;122:543-9.
  43. Abduo J, Palamara JEA. Accuracy of digital impressions versus conventional impressions for 2 implants: an in vitro study evaluating the effect of implant angulation. *Int J Implant Dent* 2021;7:75.
  44. Alikhasi M, Siadat H, Nasirpour A, Hasanzade M. Three-dimensional accuracy of digital impression versus conventional method: effect of implant angulation and connection type. *Int J Dent* 2018;2018:3761750.
  45. Lee JH, Bae JH, Lee SY. Trueness of digital implant impressions based on implant angulation and scan body materials. *Sci Rep* 2021;11:21892.
  46. Sorrentino R, Gherlone EF, Calesini G, Zarone F. Effect of implant angulation, connection length, and impression material on the dimensional accuracy of implant impressions: an in vitro comparative study. *Clin Implant Dent Relat Res* 2010;12 Suppl 1:e63-76.